Quantum Information Processing (2026) 25:215
https://doi.org/10.1007/s11128-026-05243-9

Perfect controlled bidirectional remote implementation of general unitary operators via a partially hyperentangled state

Cao Thi Bich[1] · **Nguyen Ba An**[2]

Received: 2 January 2026 / Accepted: 1 June 2026
© The Author(s), under exclusive licence to Springer Science+Business Media, LLC, part of Springer Nature 2026

Abstract
We design a new quantum circuit to generate a five-photon maximal slice state, which is partially hyperentangled in two degrees of freedom. This state is then employed as a shared quantum channel for a protocol of controlled bidirectional remote implementation of general unitary operators. In our protocol, the parameters characteristic of the quantum channel is known exclusively by the controller, Charlie; as a result, only she is able to act appropriately to decide on the completion of the protocol. The merits of our protocol are twofold: First, it extends the ability of bidirectional remote implementation of partially unknown quantum operators to general unknown unitary ones, and second, the proposed two-way common control based on hyperentanglement requires fewer resources than two one-way separate controls based on conditional entanglements do. Remarkably, our protocol is perfect (i.e., achieving a success probability and fidelity of 1), yet this perfection is independent of the quantum channel parameters (i.e., it is insensitive to the channel's entanglement degree).

Keywords Controlled bidirectional remote implementation of operators · Maximal slice hyperentangled state · Cross-Kerr nonlinearities · X-quadrature measurement

1 Introduction

Quantum entanglement [1] represents nonclassical correlations between particles and serves as a fundamental resource for quantum information processing tasks such as

✉ Cao Thi Bich
ctbich@iop.vast.vn

Nguyen Ba An
annb@thanglong.edu.vn

[1] Institute of Physics, Vietnam Academy of Science and Technology (VAST), 10 Dao Tan, Giang Vo, Hanoi, Vietnam

[2] Thang Long Institute of Mathematics and Applied Sciences (TIMAS), Thang Long University (TLU), Nghiem Xuan Yem, Dinh Cong, Hanoi, Vietnam

Published online: 12 June 2026

quantum teleportation (QT) [2, 3], quantum cryptography [4, 5] and measurement-based quantum computation [6, 7]. Among these applications, QT first proposed by Bennett et al. in 1993 [2] enables the transmission of an arbitrary unknown quantum state from a sender to a distant receiver through a pre-shared Einstein–Podolsky–Rosen (EPR) entangled pair, Bell-state measurements and classical communication. Building upon the principles of QT, Huelga et al. [8] introduced quantum remote control in 2001, a scheme based on bidirectional quantum teleportation (BQT) that enables the remote implementation of arbitrary unitary operations on unknown quantum systems with a resource cost of two entangled bits (ebits) and four classical bits (cbits). Subsequently, they demonstrated that remote implementation of operators (RIO) can be achieved more efficiently using two ebits and only three cbits, thereby motivating the development of resource-efficient protocols beyond conventional BQT methods. Moreover, they showed that when the target operators belong to restricted sets, deterministic RIO can be realized using only one ebit and two cbits [9]. Since its inception, RIO has been extensively investigated using various quantum channels and physical platforms [10–22]. Further developments incorporated quantum control into RIO, leading to controlled RIO protocols [22–26]. In these schemes, the controller is responsible not only for distributing the quantum channel among the participating parties but also for determining whether the protocol can be completed through the disclosure of measurement outcomes. Consequently, the controller plays both channel-preparation and decision-making roles, thereby enhancing the controllability and security of the remote implementation process. Therefore, the construction and distribution of the shared quantum channel must be carefully designed according to the objectives and practical requirements of the protocol.

In Ref. [22], the authors proposed three controlled bidirectional remote implementation of operations (CBRIO) protocols for partially unknown unitary operations by employing five-, seven-, and nine-qubit entangled states as quantum channels. These schemes address one-qubit, two-qubit and asymmetric cases within restricted classes of unitary operations. However, the protocols in Ref. [22] are formulated in terms of abstract qubits and rely on conventional maximally entangled states. As a result, they employ universal recovery operations and require only standard quantum gates such as CNOT and Hadamard gates. In realistic implementations, abstract qubits must be encoded into physical systems, particularly photons, owing to their robustness against decoherence and suitability for long-distance quantum communication. Conventional photonic entanglement usually exploits only a single degree of freedom (DOF), such as polarization. Nevertheless, photons naturally possess multiple accessible DOFs that can be simultaneously entangled, giving rise to hyperentanglement [27–29]. By allowing more information to be encoded per particle, hyperentangled states can improve information capacity and resource efficiency in quantum communication and computation. Consequently, hyperentanglement has become an important resource for advanced quantum information processing tasks, including complete Bell-state analysis [30–34], hyperentanglement swapping [33], entanglement concentration [35] and hyperparallel photonic quantum computation [36, 37].

Processing quantum information across multiple DOFs of a single photon requires measurement techniques that neither disturb the remaining DOFs nor destroy the photon itself. In this context, quantum nondemolition detectors based on cross-Kerr

nonlinearities have attracted considerable attention in theoretical quantum information processing schemes [38, 39]. Such detectors have been widely applied to quantum gate construction [38, 40, 41], entanglement generation [42–45], entangled state analysis [46] and entanglement concentration [47, 48]. Motivated by these developments, in this work we extend controlled bidirectional remote implementation of operations (CBRIO) protocols to realistic photonic systems by simultaneously exploiting the spatial mode (S-DOF) and polarization (P-DOF) degrees of freedom of photons. In particular, we employ a class of entangled resources known as maximal slice hyperentangled states. A distinctive feature of these states is that a projective measurement performed on one DOF can conditionally project the remaining DOFs into maximally entangled states, even though each individual DOF is initially only partially entangled. Based on this property, we first construct a five-photon maximal slice hyperentangled state that serves as the shared quantum channel among the participating parties. Using this resource, we then propose a new CBRIO protocol for arbitrary unitary operations. Unlike the scheme in Ref. [22], which is restricted to partially unknown operators belonging to predefined sets, the present protocol enables deterministic remote implementation of general unitary operators with unit success probability and unit fidelity under ideal conditions.

The remainder of this paper is organized as follows. In Sect. 2, we introduce the five-photon maximal slice hyperentangled state and describe its role as the shared quantum channel participating parties. In Sect. 3, we present the protocol for controlled bidirectional remote implementation of general unitary operators. Finally, Sect. 4 summarizes the main results and discusses possible future directions.

2 The protocol task and quantum channel design

In this section, we outline the protocol's specific task alongside the architectural design of the quantum channel. We consider a tripartite quantum system involving three spatially separated parties: Alice, Bob and Charlie. Alice and Bob are under the supervision of Charlie, who acts as the controller. The parties are restricted to local operations and classical communication (LOCC). Assume that Alice possesses a single photon, denoted a, which exhibits vertical polarization and simultaneously propagates along two distinct spatial paths labeled x_0 and x_1. That is, the quantum state of photon a is given by:

$$\left|\psi_1^{(SP)}\right\rangle_a = \left|\psi_1^{(S)}\right\rangle_a |V\rangle_a \,, \tag{1}$$

where

$$\left|\psi_1^{(S)}\right\rangle_a = \alpha\,|x_0\rangle_a + \beta\,|x_1\rangle_a \,, \tag{2}$$

with α and β being unknown complex coefficients satisfying the normalization condition $|\alpha|^2 + |\beta|^2 = 1$. The basis states $\left|x_j\right\rangle_a$ (for $j = 0, 1$) correspond to photon a traveling along path x_j, while $|V\rangle_a$ denotes the vertical polarization component.

Note that the superscript (SP) indicates both the spatial and polarization degrees of freedom (SP-DOF), while the superscript (S) refers to the S-DOF only.

Bob is equipped with a device capable of implementing an arbitrary single-qubit unitary transformation acting on the S-DOF of a single photon. The general form of the unitary operator is given by:

$$U_1^{(S)} = \begin{pmatrix} u & v \\ -v^* & u^* \end{pmatrix}, \tag{3}$$

which acts on the S-DOF of Alice's photon as follows:

$$U_1^{(S)} \left|\psi_1^{(S)}\right\rangle = \left|\psi_1'^{(S)}\right\rangle = \alpha_1 \left|x_0\right\rangle + \beta_1 \left|x_1\right\rangle, \tag{4}$$

where the output coefficients α_1 and β_1 are expressed as:

$$\alpha_1 = \alpha u - \beta v^*, \quad \beta_1 = \alpha v + \beta u^*. \tag{5}$$

Analogously, Bob possesses a photon b, which also has vertical polarization and propagates simultaneously along two spatial paths y_0 and y_1. The total state of Bob's photon is represented as:

$$\left|\psi_2^{(SP)}\right\rangle_b = \left|\psi_2^{(S)}\right\rangle_b \left|V\right\rangle_b, \tag{6}$$

where the spatial part of the state is given by:

$$\left|\psi_2^{(S)}\right\rangle_b = \gamma \left|y_0\right\rangle_b + \delta \left|y_1\right\rangle_b, \tag{7}$$

with complex coefficients γ and δ satisfying the normalization $|\gamma|^2 + |\delta|^2 = 1$.

Alice is assumed to possess a device capable of implementing a general unitary transformation $U_2^{(S)}$ on the S-DOF of a single photon, represented as:

$$U_2^{(S)} = \begin{pmatrix} s & p \\ -p^* & s^* \end{pmatrix}, \tag{8}$$

which acts on the S-DOF of Bob's photon as:

$$U_2^{(S)} \left|\psi_2^{(S)}\right\rangle = \left|\psi_2'^{(S)}\right\rangle = \gamma_1 \left|y_0\right\rangle + \delta_1 \left|y_1\right\rangle, \tag{9}$$

with transformed coefficients given by:

$$\gamma_1 = \gamma s - \delta p^*, \quad \delta_1 = \delta p + \gamma s^*. \tag{10}$$

Charlie serves as the controller in the protocol and plays a decisive role in determining the completion of the CBRIO protocol. The task of interest here is that Alice,

Bob and Charlie remotely cooperate so that, upon permission of Charlie, Alice (Bob) ultimately obtains $|\psi_1'\rangle|V\rangle$ ($|\psi_2'\rangle|V\rangle$). To accomplish this task, we find that a quantum channel of the following form would be suitable

$$\left|Q^{(SP)}\right\rangle_{12345} = \left|Q^{(S)}\right\rangle_{12345} \otimes \left|Q^{(P)}\right\rangle_{12345}. \tag{11}$$

Here,

$$\begin{aligned}\left|Q^{(S)}\right\rangle_{12345} = \frac{1}{2}\Big(&|a_0b_0c_0d_0e_0\rangle + \sin\theta_1\,|a_0b_0c_1d_1e_1\rangle + \sin\theta_1\,|a_1b_1c_0d_0e_1\rangle \\ &+ \cos\theta_1\,|a_0b_0c_1d_1e_0\rangle + \cos\theta_1\,|a_1b_1c_0d_0e_0\rangle + |a_1b_1c_1d_1e_0\rangle\Big)_{12345}\end{aligned} \tag{12}$$

and

$$\begin{aligned}\left|Q^{(P)}\right\rangle_{12345} = \frac{1}{2}\Big(&|HHHHH\rangle + \sin\theta_2\,|HHVVV\rangle + \sin\theta_2\,|VVHHV\rangle \\ &+ \cos\theta_2\,|HHVVH\rangle + \cos\theta_2\,|VVHHH\rangle + |VVVVH\rangle\Big)_{12345}.\end{aligned} \tag{13}$$

It is evident that $\left|Q^{(SP)}\right\rangle_{12345}$ constitutes a five-photon state which is entangled in both the S- and the P-DOF, but the entanglement degrees in each DOF are not maximal. Each photon simultaneously propagates along two distinct paths (photon 1 along paths a_0 and a_1, photon 2 along paths b_0 and b_1, photon 3 along paths c_0 and c_1, photon 4 along paths d_0 and d_1 and photon 5 along paths e_0 and e_1) and is in a superposition of both horizontal (H) and vertical (V) polarization. As evident from Eqs. (12) and (13), the quantum channel state is parameterized by two angles θ_1 and θ_2. The entanglement between Alice and Bob remains intact regardless of the specific values of these parameters. In contrast, the entanglement involving the controller is highly sensitive to θ_1 and θ_2. Specifically, when the sine of any of these angles vanishes, the qubit(s) held by Charlie become completely disentangled from the rest of the system, thereby nullifying his role as a quantum controller. Because of this property, the state in Eq. (11) is referred to as the maximal slice (MS) state. In particular, when the sine of both angles θ_1 and θ_2 is equal to ± 1, this entanglement reaches its maximal value. In the current setting, these angles are chosen such that the sine is neither 0 nor ± 1, resulting in a non-maximal degree of entanglement. Crucially, the parameters θ_1 and θ_2 are deliberately known only to the controller Charlie. This setting significantly enhances the protocol's security: Even if the qubits held by Alice and Bob are unexpectedly intercepted by a malicious adversary, Eve, the target state defined in Eq. (11) remains concealed. Since Eve lacks knowledge of the parameter values, she is unable to determine the appropriate recovery operations.

To construct the hyperentangled state (11), we begin with the following initial state:

$$\left|Q_0^{(SP)}\right\rangle_{12345} = \left|Q_0^{(S)}\right\rangle_{12345} \otimes \left|Q_0^{(P)}\right\rangle_{12345}. \tag{14}$$

In this expression,

$$\left|Q_0^{(S)}\right\rangle_{12345} = \frac{1}{2}\Big(|a_0b_0c_0d_0e_0\rangle + |a_0b_0c_1d_1e_1\rangle + |a_1b_1c_0d_0e_1\rangle + |a_1b_1c_1d_1e_0\rangle \Big)_{12345}, \tag{15}$$

and

$$\left|Q_0^{(P)}\right\rangle_{12345} = \frac{1}{2}\Big(|HHHHH\rangle + |HHVVV\rangle + |VVHHV\rangle + |VVVVH\rangle \Big)_{12345}. \tag{16}$$

These initial states can be prepared by the schemes proposed in our previous work [49]. To generate the target state (11) from the state (14), we divide the process into two stages: The first stage involves generating the state (12) from the state (15), and the second stage involves generating the state (13) from the state (16).

Stage 1: constructing state (12) from state (15):

This stage consists of the following three sequential steps.

Step 1: An unbalanced beam splitter UBS(θ_1) with transmission (reflection) coefficient $\cos\theta_1$ ($\sin\theta_1$) is placed in path e_1 of photon 5 that performs the transformation for the photon's S-DOF as

$$\mathrm{UBS}(\theta_1)|e_1\rangle = \sin\theta_1|e_1\rangle + \cos\theta_1|e_1'\rangle, \tag{17}$$

where e_1' is the transmitted path of mode e_1 after passing through the UBS(θ_1). As a result, the state $|Q_0^{(S)}\rangle$ evolves into

$$\begin{aligned}|Q_1^{(S)}\rangle_{12345} = \frac{1}{2}(&|a_0b_0c_0d_0e_0\rangle + \sin\theta_1|a_0b_0c_1d_1e_1\rangle + \sin\theta_1|a_1b_1c_0d_0e_1\rangle \\ &+ \cos\theta_1|a_0b_0c_1d_1e_1'\rangle + \cos\theta_1|a_1b_1c_0d_0e_1'\rangle + |a_1b_1c_1d_1e_0\rangle)_{12345}.\end{aligned} \tag{18}$$

Subsequently, we let modes e_0 and e_1' interfere at a balanced beam splitter (BBS), while mode e_1 is also sent through another BBS. This process transforms the state $|Q_1^{(S)}\rangle_{12345}$ onto

$$|Q_2^{(S)}\rangle_{12345} = \frac{1}{\sqrt{2}}\left(|Q_3^{(S)}\rangle_{12345} + |Q_4^{(S)}\rangle_{12345}\right), \tag{19}$$

where

$$\begin{aligned}|Q_3^{(S)}\rangle_{12345} = \frac{1}{2}(&|a_0b_0c_0d_0e_0\rangle + \sin\theta_1|a_0b_0c_1d_1e_1\rangle + \sin\theta_1|a_1b_1c_0d_0e_1\rangle \\ &+ \cos\theta_1|a_0b_0c_1d_1e_0\rangle + \cos\theta_1|a_1b_1c_0d_0e_0\rangle + |a_1b_1c_1d_1e_0\rangle)_{12345},\end{aligned} \tag{20}$$

and

$$|Q_4^{(S)}\rangle_{12345} = \frac{1}{2}(|a_0b_0c_0d_0e_1'\rangle + \sin\theta_1|a_0b_0c_1d_1e_2\rangle + \sin\theta_1|a_1b_1c_0d_0e_2\rangle - \cos\theta_1|a_0b_0c_1d_1e_1'\rangle - \cos\theta_1|a_1b_1c_0d_0e_1'\rangle + |a_1b_1c_1d_1e_1'\rangle)_{12345}. \quad (21)$$

Here, e_2 is the transmitted path of mode e_1 after passing through the BBS.

Next, we allow modes e_1' and e_2 of photon 5 to interact with a coherent state $|z\rangle_6$, which has a real and positive amplitude z and travels along a new path labeled 6. This interaction occurs via cross-Kerr nonlinearity, inducing phase shifts of amplitude η. A homodyne measurement is subsequently performed on the coherent state. The measurement outcome is denoted by ζ, where $\zeta = 0$ corresponds to the case in which no phase shift is detected, while $\zeta = 1$ corresponds to the case in which a phase shift has occurred.

If $\zeta = 0$, the five-photon system collapses into the state $|Q_3^{(S)}\rangle_{12345}$, which matches the desired target state. This outcome occurs with a probability of $p_{\zeta=0} = 1/2$. The operations applied to photon 5 are illustrated in the upper part of Fig. 1. In this scenario, photon 5 is routed through spatial modes e_0 and e_1. Because these primary operations are localized entirely on photon 5, photons 1 through 4 are omitted from the diagram for visual clarity.

Conversely, if $\zeta = 1$, a phase shift $e^{i\eta}$ has been detected in the coherent state $|z\rangle_6$; the system collapses into the state $|Q_4^{(S)}\rangle_{12345}$ with the same probability $p_{\zeta=1} = 1/2$. The relevant operations in this scenario are depicted in the lower part of Fig. 1, where photon 5 now travels at the same time along two alternative paths e_1' and e_2. In this case, the protocol proceeds to the next step.

Step 2: In the case where the measurement outcome is $\zeta = 1$, we proceed as follows: The modes e_0 and e_1' in Eq. (21) are interfered via a BBS. Simultaneously, modes e_1 and e_2 are interfered via another BBS. This results transform $|Q_4^{(S)}\rangle_{12345}$ into

$$|Q_5^{(S)}\rangle_{12345} = \frac{1}{\sqrt{2}}\left(|Q_6^{(S)}\rangle_{12345} + |Q_7^{(S)}\rangle_{12345}\right), \quad (22)$$

where

$$|Q_6^{(S)}\rangle_{12345} = \frac{1}{2}(|a_0b_0c_0d_0e_0\rangle + \sin\theta_1|a_0b_0c_1d_1e_1\rangle + \sin\theta_1|a_1b_1c_0d_0e_1\rangle - \cos\theta_1|a_0b_0c_1d_1e_0\rangle - \cos\theta_1|a_1b_1c_0d_0e_0\rangle + |a_1b_1c_1d_1e_0\rangle)_{12345}, \quad (23)$$

and

$$|Q_7^{(S)}\rangle_{12345} = -\frac{1}{2}(|a_0b_0c_0d_0e_1'\rangle + \sin\theta_1|a_0b_0c_1d_1e_2\rangle + \sin\theta_1|a_1b_1c_0d_0e_2\rangle - \cos\theta_1|a_0b_0c_1d_1e_1'\rangle - \cos\theta_1|a_1b_1c_0d_0e_1'\rangle + |a_1b_1c_1d_1e_1'\rangle)_{12345}. \quad (24)$$

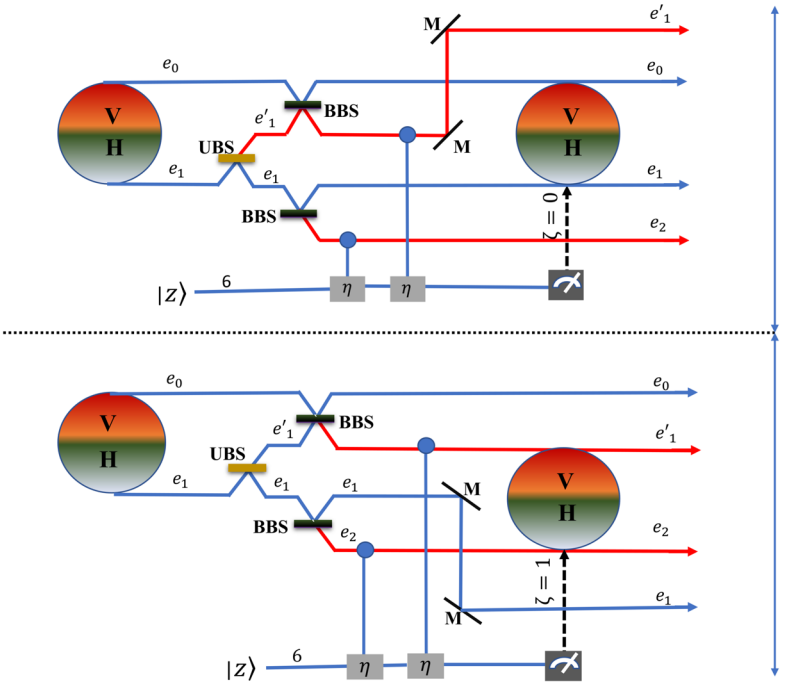

Fig. 1 Schematic illustration of the operations applied to photon 5 in step 1 of Stage 1. The upper panel corresponds to the case where the homodyne measurement yields the outcome $\zeta = 0$, indicating no phase shift in the output coherent state. In this case, photon 5 follows the path through spatial modes e_0 and e_1, and the five-photon system collapses directly into the target state $|Q^{(S)}\rangle$. The lower panel depicts the case where the measurement yields $\zeta = 1$, indicating a phase shift $e^{i\eta}$ in the output coherent state; here, photon 5 is directed through modes e'_1 and e_2, and the protocol proceeds to the next stage. For clarity, photons 1, 2, 3 and 4 are omitted since the main operations are performed solely on photon 5

Next, we let modes e'_1 and e_2 of photon 5 interact once more with a coherent state $|z\rangle_7$, which has a real, positive amplitude z and propagates along path 7. This interaction occurs via cross-Kerr nonlinearity, after which a homodyne measurement performed with the outcome denoted by ζ_1.

If $\zeta_1 = 0$, i.e., no phase shift in $|z\rangle_7$ is detected, the system collapses into the state $|Q_6^{(S)}\rangle_{12345}$ with a probability of $p_{\zeta_1=0} = \frac{1}{2} \times p_{\zeta=1} = \frac{1}{4}$. In this case, we apply the operator $Z^{(S)}$ to mode b_1 of photon 2, mode c_1 of photon 3 and mode e_1 of photon 5 to recover the target state $|Q^{(S)}\rangle$, as defined in Eq. (12). The corresponding operations acting on photon 5 that enable the transition from Eq. (15)–(12) in the specific cases where $\zeta = 1$ and $\zeta_1 = 0$ are illustrated in Fig 2. Although this step involves additional actions on photons 2 and 3, the main transformations remain localized on photon 5. For simplicity, photons 1, 2, 3 and 4 are omitted from Fig. 2.

Conversely, if $\zeta_1 = 1$, meaning a phase shift of $e^{i\eta}$ is observed in $|z\rangle_7$, the system evolves into the state $|Q_7^{(S)}\rangle_{12345}$, which occurs with probability $p_{\zeta_1=1} = \frac{1}{2} \times p_{\zeta=1} = \frac{1}{4}$. This state is equivalent to $|Q_4^{(S)}\rangle_{12345}$, and the protocol returns to Step 2.

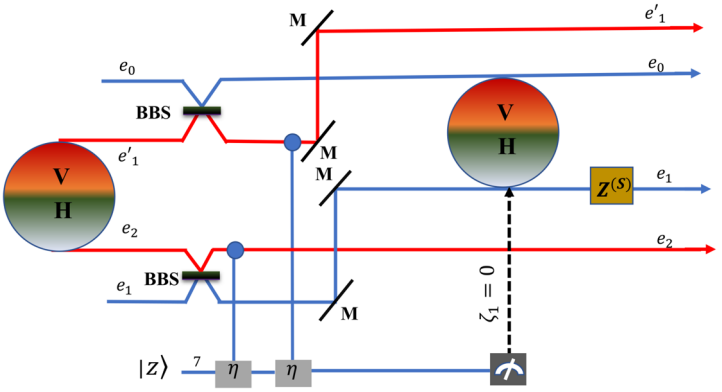

Fig. 2 Schematic illustration of the operations applied to photon 5 in step 2 of Stage 1. The figure corresponds to the case where the homodyne measurement yields the outcome $\zeta_1 = 0$, indicating no phase shift in the output coherent state. In this case, photon 5 follows the path through spatial modes e_0 and e_1, and the five-photon system collapses directly into the target state $|Q^{(S)}\rangle$

Step 3 (Recursive loop): Whenever the measurement yields $\zeta_1 = 1$, the system re-enters the intermediate state $|Q_4^{(S)}\rangle_{12345}$ and the same procedure is repeated. That is, modes e'_1 and e_2 of photon 5 again interact with a new coherent state through cross-Kerr nonlinearity, followed by homodyne detection. The loop continues until a measurement outcome $\zeta_i = 0$ is obtained at the i-th round, after which the operator $Z^{(S)}$ is applied to yield the desired state $|Q^{(S)}\rangle$.

Each iteration results in one of two equally likely outcomes. Since the initial entrance into the loop occurs with probability $p_{\zeta=1} = \frac{1}{2}$, and each subsequent trial has a success probability of $\frac{1}{2}$, the probability of successfully obtaining the target state at the i-th attempt is:

$$P_{\text{success}}^{(i)} = \left(\frac{1}{2}\right)^{i+1}, \quad \text{for } i = 0, 1, 2, \ldots \tag{25}$$

Thus, the cumulative success probability after n rounds is:

$$P_{\text{total}}^{(n)} = \sum_{i=0}^{n} \left(\frac{1}{2}\right)^{i+1} = 1 - \left(\frac{1}{2}\right)^{n+1}. \tag{26}$$

Taking the limit $n \to \infty$, we obtain:

$$\lim_{n\to\infty} P_{\text{total}}^{(n)} = 1. \tag{27}$$

This demonstrates that Stage 1 would be obtained eventually.

Stage 2: constructing state (13) from state (16):

We now consider the procedure for generating the P-DOF entangled state $\left|Q^{(P)}\right\rangle_{12345}$ in Eq. (13) from the initial state $\left|Q_0^{(P)}\right\rangle_{12345}$ in Eq. (16). This procedure also involves two steps.

Step 1: The V-polarized component of photon 5 is directed through a wave plate characterized by the rotation angle θ_2. This process is effectively equivalent to sending photon 5 through an optical setup denoted as W, which comprises two polarizing beam splitters (PBSs), a polarization wave plate set at angle θ_2 and a series of mirrors arranged as illustrated in the lower panel of Fig. 4. Following this, the spatial modes e_0 and e_0' are combined at a BBS, while the modes e_1 and e_1' interfere at another BBS. As a result, the joint state of photons 1 through 5 evolves into the following superposition:

$$|Q_1^{(SP)}\rangle_{12345} = \frac{1}{\sqrt{2}}(|\lambda_1\rangle_{12345} + |\lambda_2\rangle_{12345}). \tag{28}$$

Here,

$$\begin{aligned}|\lambda_1\rangle_{12345} = \frac{1}{4}\Big(&|a_0b_0c_0d_0e_0\rangle + \sin\theta_1|a_0b_0c_1d_1e_1\rangle + \sin\theta_1|a_1b_1c_0d_0e_1\rangle \\ &+ \cos\theta_1|a_0b_0c_1d_1e_0\rangle + \cos\theta_1|a_1b_1c_0d_0e_0\rangle + |a_1b_1c_1d_1e_0\rangle\Big)_{12345} \\ &\otimes\Big(|HHHHH\rangle + \sin\theta_2|HHVVV\rangle + \sin\theta_2|VVHHV\rangle \\ &+ \cos\theta_2|HHVVH\rangle + \cos\theta_2|VVHHH\rangle + |VVVVH\rangle\Big)_{12345}\end{aligned} \tag{29}$$

and

$$\begin{aligned}|\lambda_2\rangle_{12345} = \frac{1}{4}\Big(&|a_0b_0c_0d_0e_0'\rangle + \sin\theta_1|a_0b_0c_1d_1e_1'\rangle + \sin\theta_1|a_1b_1c_0d_0e_1'\rangle \\ &+ \cos\theta_1|a_0b_0c_1d_1e_0'\rangle + \cos\theta_1|a_1b_1c_0d_0e_0'\rangle + |a_1b_1c_1d_1e_0'\rangle\Big)_{12345} \\ &\otimes\Big(|HHHHH\rangle + \sin\theta_2|HHVVV\rangle + \sin\theta_2|VVHHV\rangle \\ &- \cos\theta_2|HHVVH\rangle - \cos\theta_2|VVHHH\rangle + |VVVVH\rangle\Big)_{12345}.\end{aligned} \tag{30}$$

Next, an ancillary coherent state $|z\rangle_8$, characterized by a real, positive amplitude z and propagating along path 8, is sequentially coupled to the spatial modes e_0' and e_1' of photon 5 via cross-Kerr nonlinear interactions. Both couplings are assumed to have the same dimensionless interaction strength η. Following these interactions, a homodyne measurement is performed on the coherent state, yielding an outcome denoted by h.

If no phase shift is detected in the coherent state $|z\rangle_8$, corresponding to the outcome $h = 0$, the coherent state remains unchanged, and the five-photon system collapses into the state $|\lambda_1\rangle_{12345}$ with a probability $p_{h=0} = 1/2$. This state is exactly the desired target state $|Q^{(SP)}\rangle_{12345}$. The associated operations acting on photon 5, which facilitate

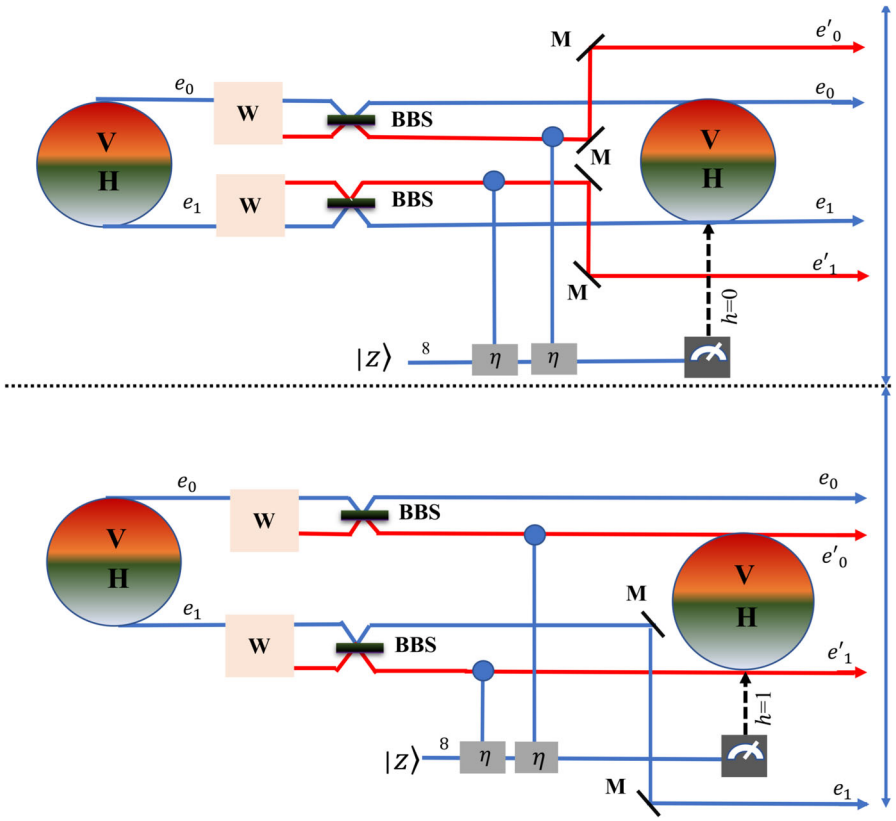

Fig. 3 Schematic illustration of the operations applied to photon 5 in step 1 of Stage 2. The upper panel corresponds to the case where the homodyne measurement yields the outcome $h = 0$, indicating no phase shift in the output coherent state. In this case, photon 5 follows the path through spatial modes e_0 and e_1, and the five-photon system collapses directly into the target state $|Q^{(SP)}\rangle$. The lower panel depicts the case where the measurement yields $h = 1$, indicating a phase shift $e^{i\eta}$ in the output coherent state; here, photon 5 is directed through modes e'_0 and e'_1, and the protocol proceeds to the next step. For clarity, photons 1, 2, 3 and 4 are omitted since the main operations are performed solely on photon 5

the transition from Eq. (16)–(13) in the specific case $h = 0$, are depicted in the upper panel of Fig. 3.

Conversely, if a phase shift of $e^{i\eta}$ is observed in the resulting coherent state corresponding to $h = 1$, the system collapses into the state $|\lambda_2\rangle_{12345}$, with the same probability $p_{h=1} = 1/2$. The associated operations acting on photon 5 in the specific case $h = 1$ are depicted in the lower panel of Fig. 3. In this situation, the protocol proceeds to the next step.

Step 2: Let spatial mode e_0 and e'_0 interfere at a BBS, and similarly, modes e_1 and e'_1 interfere through another BBS. As a result of these operations, the state of photons 1 through 5 evolves into:

$$|Q_3^{(SP)}\rangle_{12345} = \frac{1}{\sqrt{2}}\left(|\lambda_3\rangle_{12345} + |\lambda_4\rangle_{12345}\right), \tag{31}$$

where

$$
\begin{aligned}
|\lambda_3\rangle_{12345} = \frac{1}{4}\Big(&|a_0b_0c_0d_0e_0\rangle + \sin\theta_1|a_0b_0c_1d_1e_1\rangle + \sin\theta_1|a_1b_1c_0d_0e_1\rangle \\
&+ \cos\theta_1|a_0b_0c_1d_1e_0\rangle + \cos\theta_1|a_1b_1c_0d_0e_0\rangle + |a_1b_1c_1d_1e_0\rangle\Big)_{12345} \\
&\otimes \Big(|HHHHH\rangle + \sin\theta_2|HHVVV\rangle + \sin\theta_2|VVHHV\rangle \\
&- \cos\theta_2|HHVVH\rangle - \cos\theta_2|VVHHH\rangle + |VVVVH\rangle\Big)_{12345}
\end{aligned} \tag{32}
$$

and

$$
\begin{aligned}
|\lambda_4\rangle_{12345} = \frac{1}{4}\Big(&|a_0b_0c_0d_0e_0'\rangle + \sin\theta_1|a_0b_0c_1d_1e_1'\rangle + \sin\theta_1|a_1b_1c_0d_0e_1'\rangle \\
&+ \cos\theta_1|a_0b_0c_1d_1e_0'\rangle + \cos\theta_1|a_1b_1c_0d_0e_0'\rangle + |a_1b_1c_1d_1e_0'\rangle\Big)_{12345} \\
&\otimes \Big(|HHHHH\rangle + \sin\theta_2|HHVVV\rangle + \sin\theta_2|VVHHV\rangle \\
&- \cos\theta_2|HHVVH\rangle - \cos\theta_2|VVHHH\rangle + |VVVVH\rangle\Big)_{12345}.
\end{aligned} \tag{33}
$$

An ancillary coherent state $|z\rangle_9$, possessing a real and positive amplitude z and traveling along mode 9, is subsequently coupled sequentially to the spatial modes e_0' and e_1' of photon 5 via cross-Kerr nonlinear interactions. Both interactions are assumed to have identical dimensionless coupling strength η. Following these couplings, a homodyne measurement is performed on the coherent state, yielding the outcome h_1.

If no phase shift is detected ($h_1 = 0$) in the resulting coherent state, the five-photon system collapses into the state $|\lambda_3\rangle_{12345}$ with a probability of $p_{h_1=0} = 1/4$. To recover the target entangled state $|Q^{(SP)}\rangle_{12345}$, a Pauli $Z^{(P)}$ operation is applied to the P-DOF of photons 2, 3 and 5 at spatial modes b_1, c_1 and e_1, respectively. The sequence of operations on photon 5 that facilitates the transition from Eq. (16)–(13) in the cases of $h = 1$ and $h_1 = 0$ is depicted in the upper panel of Fig. 4.

Alternatively, if a phase shift $e^{i\eta}$ is observed in the resulting coherent state ($h_1 = 1$), the system collapses into the state $|\lambda_4\rangle_{12345}$, which coincides with the previously defined state $|\lambda_2\rangle_{12345}$. Whenever the measurement yields $h_1 = 1$, the system re-enters the intermediate state $|\lambda_2\rangle_{12345}$, and the same procedure is repeated. The loop continues until a measurement outcome $h_i = 0$ is obtained at the i-th round, after which the operator $Z^{(P)}$ is applied to yield the desired state $|Q^{(P)}\rangle$. This demonstrates that Stage 2 is asymptotically deterministic: After a sufficiently large number of repetitions, the target state $|Q^{(SP)}\rangle$ will eventually be obtained.

3 Perfect CBRIO via MS state

Once the MS state (11) is generated, it serves as a suitable quantum channel for the protocol of CBRIO of general unitary operators described in Sect. 2.

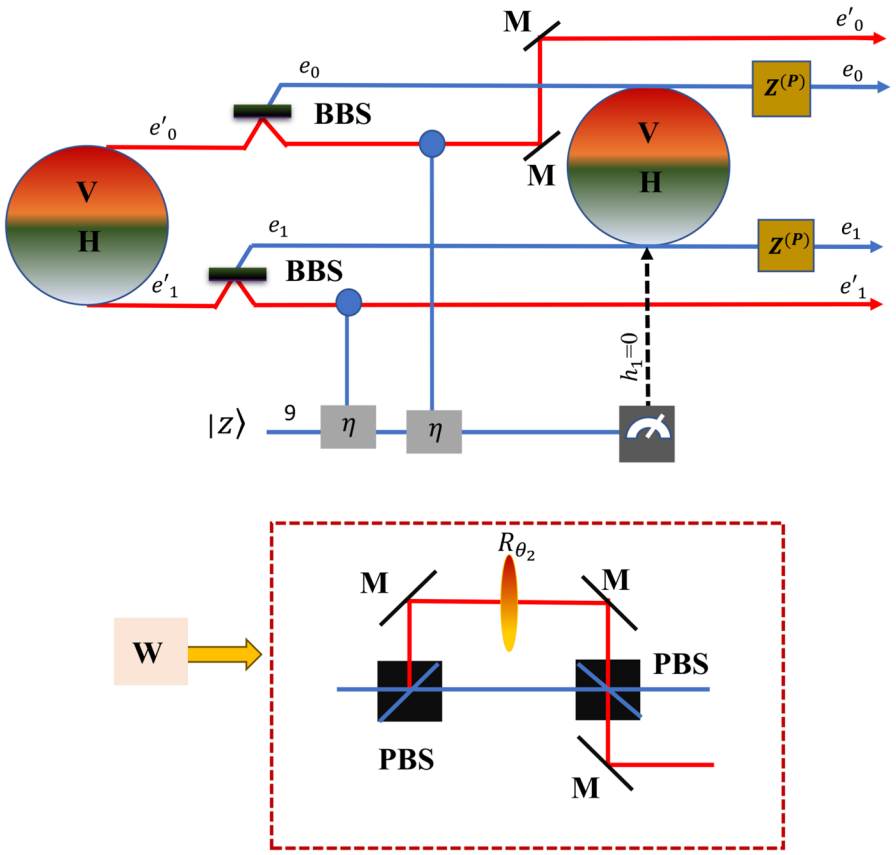

Fig. 4 Schematic illustration of the operations applied to photon 5 in step 2 of Stage 2. The figure corresponds to the case where the homodyne measurement yields the outcome $h_1 = 0$, indicating no phase shift in the output coherent state. In this case, photon 5 follows the path through spatial modes e_0 and e_1, and the five-photon system collapses directly into the target state $|Q^{(SP)}\rangle$

For clarity, we recall that our objective is to design a protocol in which Alice and Bob collaborate such that, once Charlie permits, Alice ends up holding a photon in the state given by Eq. (4), while Bob holds a photon in the state given by Eq. (9). Importantly, this is achieved using only local operations and classical communication (LOCC). This scenario can be interpreted as a controlled bidirectional remote implementation of operators protocol, where Bob remotely applies his operator $U_1^{(S)}$ to Alice's state $|\psi_1^{(SP)}\rangle$, while Alice remotely applies her operator $U_2^{(S)}$ to Bob's state $|\psi_2^{(SP)}\rangle$. To execute the CBRIO protocol using the five-photon quantum channel, Alice holds photons a, 1 and 3; Bob holds photons b, 2 and 4; and Charlie retains photon 5. The global state of the problem before execution of any operations has the form

$$|\Psi^{(SP)}\rangle_{ab12345} = |\Psi^{(S)}\rangle_{ab12345} \otimes |\Psi^{(P)}\rangle_{ab12345}, \tag{34}$$

where

$$|\Psi^{(S)}\rangle_{ab12345} = (\alpha\gamma|x_0y_0\rangle + \alpha\delta|x_0y_1\rangle + \beta\gamma|x_1y_0\rangle + \beta\delta|x_1y_1\rangle)_{ab} \otimes |Q^{(S)}\rangle_{12345} \tag{35}$$

and

$$|\Psi^{(P)}\rangle_{ab12345} = |VV\rangle_{ab} \otimes |Q^{(P)}\rangle_{12345}. \tag{36}$$

For the CBRIO protocol, we will carry out the following three steps in sequence:

Step 1: In this step, the operations are restricted to the S-DOF. Therefore, we focus solely on the component $\left|\Psi^{(S)}\right\rangle_{ab12345}$ and temporarily disregard the P-DOF part of the quantum channel. Alice and Bob act independently, while Charlie carries out the first stage of control. Their operations are illustrated in Fig. 5.

Alice begins by preparing a coherent state (CS), denoted as $|z\rangle_{\epsilon_1}$, where z is a positive real amplitude, and the state propagates along path ϵ_1. This CS is made to interact with the states $|x_0\rangle_a$ and $|a_0\rangle_1$ through the cross-Kerr mechanism, with interaction parameters η_1 and $-\eta_1$, respectively. Following these interactions, Alice performs a homodyne measurement on the resulting CS to determine its quadrature value along the X-axis. The measurement outcome is denoted by k, where $k = 0$ corresponds to the detection of the unshifted state $|z\rangle_{\epsilon_1}$ and $k = 1$ corresponds to the detection of either shifted state $|ze^{\pm i\eta_1}\rangle_{\epsilon_1}$.

Independently, Bob performs a similar procedure. He prepares a coherent state $|z\rangle_{\epsilon_2}$, propagating along path ϵ_2. This CS interacts with the states $|y_0\rangle_b$ and $|d_0\rangle_4$ via cross-Kerr interactions characterized by parameters η_2 and $-\eta_2$, respectively. After the nonlinear interactions, Bob performs a homodyne measurement to obtain the X-quadrature of the resulting CS. The measurement result is denoted by l, where $l = 0$ corresponds to the detection of $|z\rangle_{\epsilon_2}$ and $l = 1$ corresponds to the detection of $|ze^{\pm i\eta_2}\rangle_{\epsilon_2}$. Depending on the measurement outcomes k and l obtained by Alice and Bob, respectively, the state of the seven photons a, b, 1, 2, 3, 4 and 5 in the S-DOF can be written as follows:

$$\begin{aligned}\left|T_{kl}^{(S)}\right\rangle_{ab12345} = {} & f_k g_l |x_k y_l\rangle_{ab} |a_0\rangle_1 |b_0\rangle_2 |c_0\rangle_3 |d_0\rangle_4 |e_0\rangle_5 \\ & + \sin\theta_1 f_k g_{l\oplus1} |x_k y_{l\oplus1}\rangle_{ab} |a_0\rangle_1 |b_0\rangle_2 |c_1\rangle_3 |d_1\rangle_4 |e_1\rangle_5 \\ & + \sin\theta_1 f_{k\oplus1} g_l |x_{k\oplus1} y_l\rangle_{ab} |a_1\rangle_1 |b_1\rangle_2 |c_0\rangle_3 |d_0\rangle_4 |e_1\rangle_5 \\ & + \cos\theta_1 f_k g_{l\oplus1} |x_k y_{l\oplus1}\rangle_{ab} |a_0\rangle_1 |b_0\rangle_2 |c_1\rangle_3 |d_1\rangle_4 |e_0\rangle_5 \\ & + \cos\theta_1 f_{k\oplus1} g_l |x_{k\oplus1} y_l\rangle_{ab} |a_1\rangle_1 |b_1\rangle_2 |c_0\rangle_3 |d_0\rangle_4 |e_0\rangle_5 \\ & + f_{k\oplus1} g_{l\oplus1} |x_{k\oplus1} y_{l\oplus1}\rangle_{ab} |a_1\rangle_1 |b_1\rangle_2 |c_1\rangle_3 |d_1\rangle_4 |e_0\rangle_5 , \end{aligned} \tag{37}$$

with $f_0 = \alpha$, $f_1 = \beta$, $g_0 = \gamma$, $g_1 = \delta$ and $\oplus$ an addition mod 2. There are four possible combinations of the measurement outcomes k and l, namely $kl = 00, kl = 01, kl = 10$

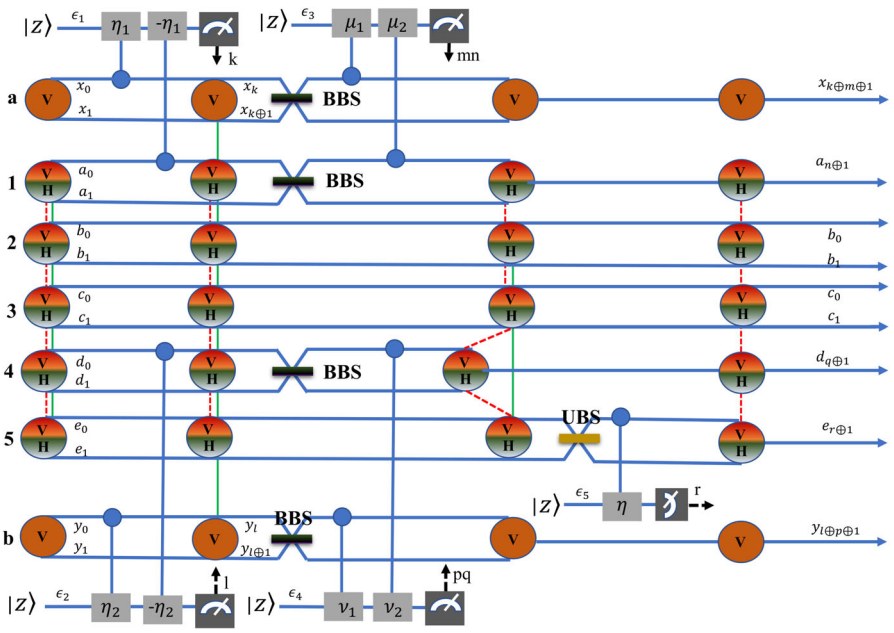

Fig. 5 Illustration of Alice, Bob and Charlie's operations in Step 1 of the CBRIO protocol on the photon state in the spatial S-DOF. Circles with two or one attached lines represent photons propagating along two or one path(s), respectively. Labels **V,H** and **V** indicate superpositions of polarization states $|V\rangle$ and $|H\rangle$, and vertical polarization $|V\rangle$, respectively. $|z\rangle$ denotes a coherent state with real positive amplitude z. BBS stands for balanced beam splitter, while UBS denotes an unbalanced beam splitter. The parameters η, $\pm\eta_1$, $\pm\eta_2$, μ_1, μ_2, ν_1 and ν_2 represent dimensionless cross-Kerr interaction strengths. Bold arrows indicate classical communication with outcomes k, l, mn, pq and r. Solid and dashed lines represent entanglement in S-DOF and P-DOF, respectively

and $kl = 11$. Each occurs with a probability of

$$P_{kl}^{(S)} = \frac{1}{4}. \tag{38}$$

Inspecting state (37) reveals that the coefficients α, β of photon a and γ, δ of photon b have been embedded into the entangled state of the seven photons a, b, 1, 2, 3, 4 and 5. The second task of Alice and Bob in this step is essentially the reverse of the first one, aiming to disentangle photons a, b, 1 and 4 from the three remaining photons 2, 3 and 5 in S-DOF. To achieve this, Alice first performs an interference experiment by sending two modes $|x_k\rangle_a$ and $|x_{k\oplus1}\rangle_a$ of photon a through a BBS, and also simultaneously sending two modes $|a_0\rangle_1$ and $|a_1\rangle_1$ of photon 1 through another BBS. Subsequently, Alice uses a different CS $|z\rangle_{\epsilon_3}$ and activates cross-Kerr mechanism with interaction parameters μ_1 and μ_2 with the modes $|x_k\rangle_a$ and $|a_0\rangle_1$, respectively. After the nonlinear interactions, Alice performs a homodyne measurement on the resulting CS to determine its phase associated with the found X-quadrature value. The homodyne measurement may detect a CS $|ze^{i(m\mu_1+n\mu_2)}\rangle_{\epsilon_3}$ for $m, n \in \{0, 1\}$, while Bob first performs an interference experiment by sending two modes $|y_l\rangle_b$ and $|y_{l\oplus1}\rangle_b$ of

photon b through a BBS, and also simultaneously sending two modes $|d_0\rangle_4$ and $|d_1\rangle_4$ of photon 4 through another BBS. Subsequently, Bob uses a different CS $|z\rangle_{\epsilon_4}$ and activates cross-Kerr mechanism with interaction parameters ν_1 and ν_2 with the modes $|y_l\rangle_b$ and $|d_0\rangle_4$, respectively. After the nonlinear interactions, Bob performs a homodyne measurement on the resulting CS to determine its phase associated with the found X-quadrature value. The homodyne measurement may detect a CS $|ze^{i(p\nu_1+q\nu_2)}\rangle_{\epsilon_4}$ for $p, q \in \{0, 1\}$. Depending on the outcomes of k, l, m, n, p and q, the seven photons are projected onto the state

$$\begin{aligned}\left|\Lambda^{(S)}_{klmnpq}\right\rangle_{ab12345} = {} & |x_{k\oplus m\oplus 1}\rangle_a \, |a_{n\oplus 1}\rangle_1 \left|y_{l\oplus p\oplus 1}\right\rangle_b \left|d_{q\oplus 1}\right\rangle_4 \Big[\\ & f_k g_l \, |b_0\rangle_2 \, |c_0\rangle_3 \, |e_0\rangle_5 \\ & + (-1)^{p\oplus q\oplus l} \sin\theta_1 \, f_k g_{l\oplus 1} \, |b_0\rangle_2 \, |c_1\rangle_3 \, |e_1\rangle_5 \\ & + (-1)^{m\oplus n\oplus k} \sin\theta_1 \, f_{k\oplus 1} g_l \, |b_1\rangle_2 \, |c_0\rangle_3 \, |e_1\rangle_5 \\ & + (-1)^{p\oplus q\oplus l} \cos\theta_1 \, f_k g_{l\oplus 1} \, |b_0\rangle_2 \, |c_1\rangle_3 \, |e_0\rangle_5 \\ & + (-1)^{m\oplus n\oplus k} \cos\theta_1 \, f_{k\oplus 1} g_l \, |b_1\rangle_2 \, |c_0\rangle_3 \, |e_0\rangle_5 \\ & + (-1)^{m\oplus n\oplus k\oplus p\oplus q\oplus l} \, f_{k\oplus 1} g_{l\oplus 1} \, |b_1\rangle_2 \, |c_1\rangle_3 \, |e_0\rangle_5 \Big]. \end{aligned} \tag{39}$$

There are 64 possible combinations of the measurement outcomes k, l, m, n, p and q, each occurring with an equal probability given by

$$P^{(S)}_{klmnpq} = \frac{1}{64}. \tag{40}$$

After the operations of Alice and Bob in Step 1, photons a, b, 1 and 4 are disentangled in the S-DOF from photons 2, 3 and 5, while all five photons 1, 2, 3, 4 and 5 remain entangled in the P-DOF. Note that since the state of photons a and b is completely separated from the other photons, we can disregard those photons from now on as they no longer play a role in next steps. The final operation in Step 1 is performed by Charlie, who knows the value of the parameter θ_1. Specifically, Charlie directs modes e_0 and e_1 to interfere via an unbalanced beam splitter UBS($\theta_1/2$), which acts as follows

$$\mathrm{UBS}(\theta_1/2)|e_0\rangle = \cos\left(\frac{\theta_1}{2}\right)|e_0\rangle + \sin\left(\frac{\theta_1}{2}\right)|e_1\rangle, \tag{41}$$

and

$$\mathrm{UBS}(\theta_1/2)|e_1\rangle = -\sin\left(\frac{\theta_1}{2}\right)|e_0\rangle + \cos\left(\frac{\theta_1}{2}\right)|e_1\rangle. \tag{42}$$

He then activates an interaction between mode e_0 and a CS $|z\rangle_{\epsilon_5}$ via the cross-Kerr nonlinearity, characterized by the parameter φ. After the interaction, Charlie measures the X-quadrature of the resulting CS. The measurement result can be $r = 0$ if the CS

remains unchanged, which occurs with probability

$$p_{r=0} = \cos^2(\theta_1/2). \tag{43}$$

Otherwise, the result is $r = 1$ if the CS evolves into $\left|ze^{i\varphi}\right\rangle_{\epsilon_5}$ with probability

$$p_{r=1} = \sin^2(\theta_1/2). \tag{44}$$

Explicitly, obtaining an outcome r projects the S-DOF state of photons 1, 2, 3, 4 and 5 onto

$$\begin{aligned}\left|\Theta^{(S)}_{klmnpqr}\right\rangle_{12345} = |a_{n\oplus1}\rangle_1 |d_{q\oplus1}\rangle_4 (f_k |b_0\rangle_2 \\ +(-1)^{k\oplus m\oplus n\oplus r\oplus1} f_{k\oplus1} |b_1\rangle_2)(g_l |c_0\rangle_3 \\ +(-1)^{l\oplus p\oplus q\oplus r\oplus1} g_{l\oplus1} |c_1\rangle_3) |e_{r\oplus1}\rangle_5 .\end{aligned} \tag{45}$$

At the end of step 1, the initial α, β coefficients in photon a and γ, δ coefficients in photon b have been successfully transferred to the S-DOF component of photon 2 and 3, respectively.

Step 2: This step focuses on the local operations performed by Alice and Bob, whose implementation procedure is illustrated in Fig. 6. After receiving the outcomes k, m, n announced by Alice and r by Charlie, Bob applies

$$R_B^{(S)} = X^k Z^{k\oplus m\oplus n\oplus r\oplus1} \tag{46}$$

on photon 2. Note that the operator $R_B^{(S)}$ only acts on the S-DOF of photon B. While after receiving the outcomes l, p, q announced by Bob and r by Charlie, Alice applies

$$R_A^{(S)} = X^l Z^{l\oplus p\oplus q\oplus r\oplus1} \tag{47}$$

on photon 3. After these operations by Bob and Alice, the state $\left|\Theta^{(S)}_{klmnpqr}\right\rangle_{12345}$ changes to

$$\begin{aligned}\left|\Sigma^{(S)}_{nqr}\right\rangle_{12345} = |a_{n\oplus1}\rangle_1 |d_{q\oplus1}\rangle_4 (\alpha |b_0\rangle_2 + \beta |b_1\rangle_2)(\gamma |c_0\rangle_3 \\ +\delta |c_1\rangle_3) |e_{r\oplus1}\rangle_5 .\end{aligned} \tag{48}$$

Then, Bob implements the operator $U_1^{(S)}$ in Eq. (3) on photon 2, while Alice implements the operator $U_2^{(S)}$ in Eq. (8) on photon 3, bringing $\left|\Sigma^{(S)}_{nqr}\right\rangle_{12345}$ to

$$\begin{aligned}\left|\chi^{(S)}_{nqr}\right\rangle_{12345} = |a_{n\oplus1}\rangle_1 |d_{q\oplus1}\rangle_4 (\alpha_1 |b_0\rangle_2 + \beta_1 |b_1\rangle_2)(\gamma_1 |c_0\rangle_3 \\ +\delta_1 |c_1\rangle_3) |e_{r\oplus1}\rangle_5 .\end{aligned} \tag{49}$$

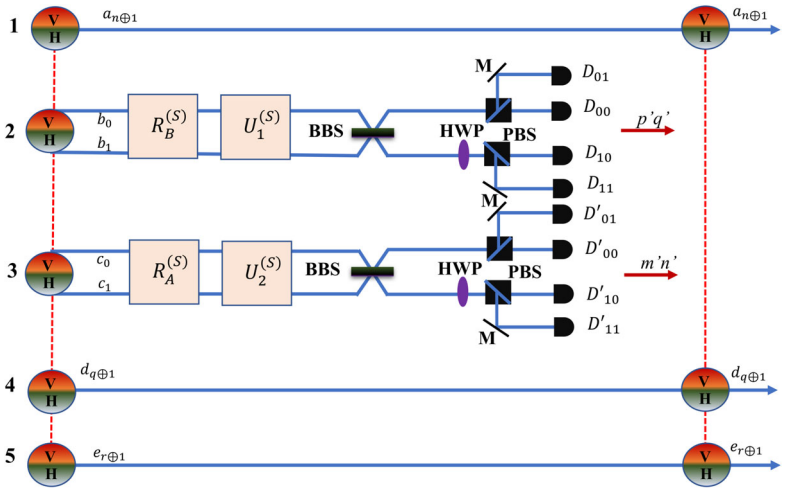

Fig. 6 The operations of Bob and Alice on photons 2 and 3, respectively, in Step 2 of CBRIO protocol. The operators $R_B^{(S)}$, $R_A^{(S)}$, $U_1^{(S)}$ and $U_2^{(S)}$ are defined in Eqs. (46), (47), (3) and (8), respectively. HWP denotes a half-wave plate, PBS is a polarization beam splitter, and M indicates a mirror, while $D_{p'q'}$ and $D_{m'n'}$ are photodetectors

At this point, the P-DOF component of the quantum channel needs to be taken into account. The full state of the five photons 1, 2, 3, 4 and 5 will be $\left|\Omega_{nqr}^{(SP)}\right\rangle_{12345} \equiv \left|\Omega_{nqr}^{(SP)}\right\rangle$

$$\begin{aligned}\left|\Omega_{nqr}^{(SP)}\right\rangle =& \frac{1}{2}[|a_{n\oplus1}H\rangle_1(\alpha_1|b_0H\rangle + \beta_1|b_1H\rangle)_2(\gamma_1|c_0H\rangle + \delta_1|c_1H\rangle)_3 \\ &\otimes |d_{q\oplus1}H\rangle_4|e_{r\oplus1}H\rangle_5 \\ &+ \sin\theta_2|a_{n\oplus1}H\rangle_1(\alpha_1|b_0H\rangle + \beta_1|b_1H\rangle)_2(\gamma_1|c_0V\rangle + \delta_1|c_1V\rangle)_3 \\ &\otimes |d_{q\oplus1}V\rangle_4|e_{r\oplus1}V\rangle_5 \\ &+ \sin\theta_2|a_{n\oplus1}V\rangle_1(\alpha_1|b_0V\rangle + \beta_1|b_1V\rangle)_2(\gamma_1|c_0H\rangle + \delta_1|c_1H\rangle)_3 \\ &\otimes |d_{q\oplus1}H\rangle_4|e_{r\oplus1}V\rangle_5 \\ &+ \cos\theta_2|a_{n\oplus1}H\rangle_1(\alpha_1|b_0H\rangle + \beta_1|b_1H\rangle)_2(\gamma_1|c_0V\rangle + \delta_1|c_1V\rangle)_3 \\ &\otimes |d_{q\oplus1}V\rangle_4|e_{r\oplus1}H\rangle_5 \\ &+ \cos\theta_2|a_{n\oplus1}V\rangle_1(\alpha_1|b_0V\rangle + \beta_1|b_1V\rangle)_2(\gamma_1|c_0H\rangle + \delta_1|c_1H\rangle)_3 \\ &\otimes |d_{q\oplus1}H\rangle_4|e_{r\oplus1}H\rangle_5 \\ &+ |a_{n\oplus1}V\rangle_1(\alpha_1|b_0V\rangle + \beta_1|b_1V\rangle)_2(\gamma_1|c_0V\rangle + \delta_1|c_1V\rangle)_3 \\ &\otimes |d_{q\oplus1}H\rangle_4|e_{r\oplus1}H\rangle_5]. \end{aligned} \tag{50}$$

Next, Bob places a half-wave plate (HWP) on path b_1 to flip the polarization of photon 2, ($|H\rangle \leftrightarrow |V\rangle$), and then mixes the spatial modes $|b_0\rangle$ and $|b_1\rangle$ on a BBS. He subsequently measures photon 2 in the basis $\{|V, b_1\rangle, |V, b_0\rangle, |H, b_1\rangle, |H, b_0\rangle\}$, using polarization beam splitters (PBSs) on both paths b_0 and b_1. Behind each PBS, that transmits horizontally polarized photons and reflects vertically polarized ones, there

are four photodetectors labeled D_{00}, D_{01}, D_{10} and D_{11}. A detection event (click) in one of these detectors reveals the outcome, and Bob communicates two classical bits $p'q' = 00, 01, 10$ or 11, corresponding to the firing of D_{00}, D_{01}, D_{10} or D_{11}.

Meanwhile, Alice places a HWP on path c_1 to flip the polarization $|H\rangle_3 \leftrightarrow |V\rangle_3$ followed by mixing $|c_0\rangle_3$ and $|c_1\rangle_3$ at a BBS. After that, she performs a measurement on photon 3 in the basis $\{|V, c_1\rangle, |V, c_0\rangle, |H, c_1\rangle, |H, c_0\rangle\}$ by using a PBS placed on each of the two paths c_0 and c_1. Behind the PBSs, there are four photodetectors labeled D'_{00}, D'_{01}, D'_{10} and D'_{11}. Depending on which detector fires, Alice reveals two classical bits $m'n'$, corresponding to the outcomes 00, 01, 10 or 11 for detectors D'_{00}, D'_{01}, D'_{10} or D'_{11}, respectively. After a fire of a photodetector, photons 2 and 3 disappear, but photons 1, 4 and 5 survive in a SP-DOF entangled state

$$\begin{aligned}\left|\Phi^{(SP)}_{nqrm'n'p'q'}\right\rangle_{145} =& f_{q'}g_{n'}|a_{n\oplus 1}H\rangle_1|d_{q\oplus 1}H\rangle_4|e_{r\oplus 1}H\rangle_5 \\ &+ (-1)^{m'}\sin\theta_2 f_{q'}g_{n'\oplus 1}|a_{n\oplus 1}H\rangle_1|d_{q\oplus 1}V\rangle_4|e_{r\oplus 1}V\rangle_5 \\ &+ (-1)^{p'}\sin\theta_2 f_{q'\oplus 1}g_{n'}|a_{n\oplus 1}V\rangle_1|d_{q\oplus 1}H\rangle_4|e_{r\oplus 1}V\rangle_5 \\ &+ (-1)^{m'}\cos\theta_2 f_{q'}g_{n'\oplus 1}|a_{n\oplus 1}H\rangle_1|d_{q\oplus 1}V\rangle_4|e_{r\oplus 1}H\rangle_5 \\ &+ (-1)^{p'}\cos\theta_2 f_{q'\oplus 1}g_{n'}|a_{n\oplus 1}V\rangle_1|d_{q\oplus 1}H\rangle_4|e_{r\oplus 1}H\rangle_5 \\ &+ (-1)^{p'\oplus m'} f_{q'\oplus 1}g_{n'\oplus 1}|a_{n\oplus 1}V\rangle_1|d_{q\oplus 1}V\rangle_4|e_{r\oplus 1}H\rangle_5, \end{aligned} \tag{51}$$

with $f_{q'} = \alpha_1$ if $q' = 0$, $f_{q'} = \beta_1$ if $q' = 1$, $g_{n'} = \gamma_1$ if $n' = 0$ and $g_{n'} = \delta_1$ if $n' = 1$.

Step 3: Step 3 comprises two key tasks: The first task involves the second stage of control carried out by Charlie in the protocol. The second involves the recovery of the target state by Alice and Bob.

Regarding Charlie's actions, he/she first inserts a wave plate $R_{\theta_2/2}$ into mode $e_{r\oplus 1}$. This wave plate transforms the horizontal and vertical polarization states according to the following rules:

$$R_{\theta_2/2}|H\rangle = \cos\left(\frac{\theta_2}{2}\right)|H\rangle + \sin\left(\frac{\theta_2}{2}\right)|V\rangle, \tag{52}$$

and

$$R_{\theta_2/2}|V\rangle = -\sin\left(\frac{\theta_2}{2}\right)|H\rangle + \cos\left(\frac{\theta_2}{2}\right)|V\rangle. \tag{53}$$

He then places a PBS in the same mode and installs a photodetector behind it to analyze the polarization state of photon 5. If photon 5 is found in the horizontal polarization state $|H\rangle$, which occurs with probability $p_{s=0} = \cos^2(\theta_2/2)$, Charlie communicates the classical bit $s = 0$. Conversely, if the photon is found in the vertical polarization state $|V\rangle$, which happens with probability $p_{s=1} = \sin^2(\theta_2/2)$, he reports $s = 1$.

Based on the outcomes n, q, n', m', p', q' and s, photons 1 and 4 will be projected to the following state:

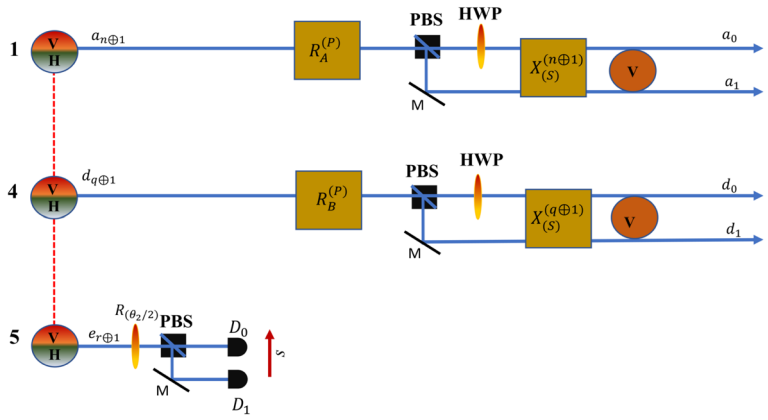

Fig. 7 Charlie's, Bob's and Alice's operations in step 3 of the CBRIO protocol. $R_{\theta_2/2}$ denotes a wave plate which acts as in Eqs. (52) and (53). $R_A^{(P)} = X_P^{q'} Z_P^{p'\oplus s\oplus1}$. $R_B^{(P)} = X_P^{n'} Z_P^{m'\oplus s\oplus1}$

$$|\Xi_{nqn'm'p'q's}\rangle_{14} = (f_{q'}|a_{n\oplus1}H\rangle + (-1)^{p'\oplus s\oplus1} f_{q'\oplus1}|a_{n\oplus1}V\rangle)_1 \\ (g_{n'}|d_{q\oplus1}H\rangle + (-1)^{m'\oplus s\oplus1} g_{n'\oplus1}|d_{q\oplus1}V\rangle)_4. \quad (54)$$

The final operations of the CBRIO protocol using non-maximally hyperentangled state are executed by Alice and Bob. Alice's operations are depicted in Fig. 7. First, she applies the operator $R_A^{(P)} = X_P^{q'} Z_P^{p'\oplus s\oplus1}$ to photon 1. It should be noted that the operator $R_A^{(P)}$ operates on P-DOF of photon 1. Next, she places a PBS in mode $a_{n\oplus1}$. Second, she places a HWP in mode $a_{n\oplus1}$ to transform $|H\rangle$ polarization into $|V\rangle$ polarization, $|\Xi'_n\rangle_1 = (\alpha_1|a_{n\oplus1}V\rangle + \beta_1|a_nV\rangle)_1$. Finally, she applies the operator $X_S^{(n\oplus1)}$, which acts on S-DOF to photon 1 to obtain the desired state, $|\psi'_1\rangle_1|V\rangle_1 = (\alpha_1|a_0\rangle + \beta_1|a_1\rangle)_1|V\rangle_1$. Parallel to this, Bob applies the operator $R_B^{(P)} = X_P^{n'} Z_P^{m'\oplus s\oplus1}$, which acts on the P-DOF of photon 4. Next, he places a PBS in mode $d_{q\oplus1}$. Secondly, he places a HWP in mode $d_{q\oplus1}$ to transform $|H\rangle$ polarization into $|V\rangle$ polarization, $|\Xi'_q\rangle_4 = (\gamma_1|d_{q\oplus1}V\rangle + \delta_1|d_qV\rangle)_4$. Finally, he applies the operator $X_S^{(q\oplus1)}$ to photon 4 to obtain the desired state, $|\psi'_2\rangle_4|V\rangle_4 = (\gamma_1|d_0\rangle + \delta_1|d_1\rangle)_4|V\rangle_4$.

4 Conclusion

The remote implementation of quantum operations is essential for the development of large-scale quantum networks. It allows quantum operations to be performed across spatially separated nodes, thereby enabling scalable quantum information processing and distributed quantum computing. By employing hyperentangled states as quantum channels, RIO and RIO-related protocols can support simultaneous operations in multiple DOFs, thereby significantly increasing channel capacity and enabling more

efficient and adaptable quantum architectures. In this work, we construct a five-photon MS state of the form in Eq. (11) which is partially entangled in both S-DOF and P-DOF. Using such state as a shared quantum channel, we propose a CBRIO protocol involving three parties: Alice, Bob and Charlie. In this protocol, Charlie holds only photon 5 of the state (11), yet he plays a decisive role in controlling two independent processes simultaneously. At this point, it is apt to observe that the CBRIO protocol could otherwise be implemented using two separate CRIO ones, each of which needs three photons so that the total quantum resource costs six photons. In contrast, our protocol achieves the same bidirectional task using a single five-photon hyperentangled state, thereby reducing the required number of physical photons from six to five. This resource reduction is significant in the scalability sense when a huge number of RIO is to be processed for a quantum algorithm.

The MS state is a multipartite entangled state in quantum information theory with the characteristic property that a projective measurement on one qubit, performed in an appropriate basis, can collapse the remaining qubits into maximally entangled states. This feature makes MS states particularly useful in quantum communication protocols where a controller plays an essential role, such as controlled quantum teleportation, controlled remote implementation of operations and quantum secret sharing. In addition, their structure allows a flexible and fine-grained distribution of entanglement, which is valuable for scalable and secure quantum networks. In our scheme, we employ a non-maximally hyperentangled state characterized by two parameters, θ_1 and θ_2. Importantly, these parameters are assumed to be known only to the controller Charlie. In contrast to protocols based on maximally entangled states, whose parameters are fixed and publicly known, the hidden-parameter structure in our protocol introduces an additional layer of control. As a consequence, except Charlie, who knows the parameters of the used non-maximally hyperentangled state, nobody else is able to correctly control the successful execution of the task. Thus, the controller's authority, the protocol security and flexibility of our protocol are enhanced compared to those in maximal-entanglement-based schemes. It can be observed that when $\theta_1 = \theta_2 = 0$, photon 5 becomes completely disentangled from the remaining subsystem, and the controller's role disappears. Conversely, for nonzero values of θ_1 and θ_2, Charlie actively governs the protocol through his measurements in Steps 1 and 3. In this case, his announcements ensure that Alice and Bob can complete the task with unit success probability and fidelity. Furthermore, Charlie's measurement on photon 5 projects photons 1–4 into two entangled pairs, $(1, 2)$ and $(3, 4)$, which is the key operational feature of the MS structure. The evaluation of the controller Charlie's role can be based on calculating the amount of information that Alice and Bob receive from each other in the absence of Charlie's active participation. We intend to carry out this calculation in a subsequent work.

By the way, we note that, upon completion of this work, a recently published paper by Ma et al. [50] addressing the same task came to our attention. In their scheme, two independent five-qubit entangled states (i.e., ten qubits in total) are required and implementation of the bidirectional control is realized through two separate controlled teleportation processes. Accordingly, the controller must manage two qubits associated with distinct entangled resources, and the protocol effectively operates via two independent quantum channels. In contrast, our scheme employs a single unified five-

photon hyperentangled MS state, where each photon encodes two degrees of freedom (spatial and polarization). This allows multiple logical qubits to be embedded within the same physical photon system, so that both directions of the remote operator implementation and the control process are integrated within one and the same entangled resource. As a result, the same task can be accomplished with fewer physical particles, since a single hyperentangled structure replaces multiple independent entangled states. Therefore, the use of hyperentanglement leads to a significant reduction in physical resources by exploiting additional degrees of freedom within each photon, while preserving the full functionality of bidirectional controlled remote implementation. Importantly, although both approaches support an arbitrary unitary operator with determinism and unit fidelity under ideal conditions, ours takes advantage of a more compact entanglement architecture, thereby boosting resource efficiency and enhancing scalability for distributed quantum information processing and quantum computation.

To end, we stress that the present protocol is primarily a theoretical one. Its implementation relies on cross-Kerr nonlinearities and homodyne measurements, which remain experimentally challenging due to the extremely weak nonlinear response at the single-photon level and unavoidable photon loss. In realistic conditions, such imperfections, together with decoherence in optical channels and detector inefficiencies, may degrade the fidelity and success probability of the protocol. At the current stage, these limitations prevent a direct experimental realization of our scheme. Nevertheless, ongoing advances in nonlinear optics, quantum measurement techniques and integrated photonic technologies are steadily improving the feasibility of such ingredients. We therefore hope that our work may serve as a useful theoretical reference and that future technological progress will enable experimental demonstrations of similar protocols.

Author Contributions The authors contributed equally to this work

Funding This work is supported by the Vietnam Academy of Science and Technology under Grant No. NVKN05.01/26-27.

Data Availability No datasets were generated or analyzed during the current study.

Materials Availability Not applicable.

Code Availability Not applicable.

Declarations

Conflict of interest The authors declare that they have no conflict of interest.

Ethical approval and consent to participate Not applicable.

References

1. Schrödinger, E.: Die gegenwärtige Situation in der Quantenmechanik. Naturwissenschaften **23**, 807 (1935)

2. Bennett, C.H., Brassard, G., Crépeau, C., Jozsa, R., Peres, A., Wootters, W.K.: Teleporting an unknown quantum state via dual classical and Einstein–Podolsky–Rosen channels. Phys. Rev. Lett. **70**, 1895 (1993)
3. Bouwmeester, D., Pan, J.W., Mattle, K., Eibl, M., Weinfurter, H., Zeilinger, A.: Experimental quantum teleportation. Nature **390**, 575 (1997)
4. Bennett, C.H., Brassard, G.: Quantum cryptography: Public key distribution and coin tossing. In: Proc. IEEE Int. Conf. on Computers, Systems and Signal Processing, pp. 175–179. (1984)
5. Ekert, A.K.: Quantum cryptography based on Bell's theorem. Phys. Rev. Lett. **67**, 661 (1991)
6. Raussendorf, R., Briegel, H.J.: A one-way quantum computer. Phys. Rev. Lett. **86**, 5188 (2001)
7. Raussendorf, R., Browne, D.E., Briegel, H.J.: Measurement-based quantum computation on cluster states. Phys. Rev. A **68**, 022312 (2003)
8. Huelga, S.F., Plenio, M.B., Vaccaro, J.A.: Quantum remote control: teleportation of unitary operations. Phys. Rev. A **65**, 042316 (2002)
9. Huelga, S.F., Plenio, M.B.: Remote control of restricted sets of operations: teleportation of angles. Phys. Rev. A **63**, 042303 (2001)
10. Yang, C.P., Gea-Banacloche, J.: Teleportation of rotations and receiver-encoded secret sharing. J. Opt. B: Quantum Semiclass. Opt. **3**, 407 (2001)
11. Collins, D., Linden, N., Popescu, S.: Nonlocal content of quantum operations. Phys. Rev. A **64**, 032302 (2001)
12. Huang, Y.F., Ren, X.F., Zhang, Y.S., Duan, L.M., Guo, G.C.: Experimental teleportation of a quantum controlled-NOT gate. Phys. Rev. Lett. **93**, 240501 (2004)
13. Xiang, G.Y., Li, J., Guo, G.C.: Teleporting a rotation on remote photons. Phys. Rev. A **71**, 044304 (2005)
14. Wang, A.M.: Remote implementations of partially unknown quantum operations of multiqubits. Phys. Rev. A **74**, 032317 (2006)
15. An, N.B.: Remote application of hidden operators. Phys. Lett. A **364**, 198 (2007)
16. Situ, H.Z., Qiu, D.W.: Investigating the implementation of restricted sets of multiqubit operations on distant qubits: a communication complexity perspective. Quantum Inf. Process. **10**, 609 (2011)
17. Peng, J.Y., He, Y.: Cyclic controlled remote implementation of partially unknown quantum operations. Int. J. Theor. Phys. **58**, 3065 (2019)
18. An, N.B.: Joint remote implementation of operators. J. Phys. A: Math. Theor. **55**, 395304 (2022)
19. Peng, J.Y., Tang, L., Yang, Z.: Deterministic hierarchical quantum operation sharing with five-qubit partially entangled states. Quantum Inf. Process. **22**, 265 (2023)
20. Kumar, S., Gangwar, K., Pathak, A.: Remote implementation of hidden or partially unknown quantum operators using optimal resources: a generalized view. Phys. Scr. **99**, 115106 (2024)
21. Jing, R., Lan, Q., Zhou, P.: Hierarchical controlled joint remote implementation of the partially unknown operations of m qudits via m high-dimensional entangled states. Entropy **26**, 857 (2024)
22. Liu, M., Maihemuti, N., Peng, J.Y.: Controlled bidirectional remote implementations of partially unknown quantum operations. Phys. Scr. **99**, 045109 (2024)
23. Wang, A.M.: Combined and controlled remote implementations of partially unknown quantum operations of multiqubits using Greenberger–Horne–Zeilinger states. Phys. Rev. A **75**, 062323 (2007)
24. Chen, L.B., Liu, Y.H., Lu, H.: Controlled and remote implementation of a split quantum rotation and sender-encoded secret sharing. Mod. Phys. Lett. B **24**, 431 (2010)
25. Zhan, Y.B., Li, X.W., Ma, P.C., Shi, J.: Controlled remote implementation of quantum operations with high-dimensional systems. Chin. Phys. B **22**, 040306 (2013)
26. He, Y.H., Lu, Q.C., Liao, Y.M., Qin, X.C., Qin, J.S., Zhou, P.: Bidirectional controlled remote implementation of an arbitrary single qubit unitary operation with EPR and cluster states. Int. J. Theor. Phys. **54**, 1726 (2015)
27. Kwiat, P.G.: Hyper-entangled states. J. Mod. Opt. **44**, 2173 (1997)
28. Barbieri, M., Cinelli, C., De Martini, F., Mataloni, P.: Photon entanglement with multiple degrees of freedom. Phys. Rev. A **72**, 052110 (2005)
29. Barreiro, J.T., Langford, N.K., Peters, N.A., Kwiat, P.G.: Generation of hyperentangled photon pairs. Phys. Rev. Lett. **95**, 260501 (2005)
30. Schuck, C., Huber, G., Kurtsiefer, C., Weinfurter, H.: Complete deterministic linear optics Bell state analysis. Phys. Rev. Lett. **96**, 190501 (2006)
31. Barreiro, J.T., Wei, T.C., Kwiat, P.G.: Beating the channel capacity limit for linear photonic superdense coding. Nat. Phys. **4**, 282 (2008)

32. Sheng, Y.B., Deng, F.G., Long, G.L.: Complete hyperentangled-Bell-state analysis for quantum communication. Phys. Rev. A **82**, 032318 (2010)
33. Ren, B.C., Wei, H.R., Hua, M., Li, T., Deng, F.G.: Complete hyperentangled-Bell-state analysis for photon systems assisted by quantum-dot spins in optical microcavities. Opt. Express **20**, 24664 (2012)
34. Wang, T.J., Lu, Y., Long, G.L.: Generation and complete analysis of the hyperentangled Bell state for photons assisted by quantum-dot spins in optical microcavities. Phys. Rev. A **86**, 042337 (2012)
35. Ren, B.C., Du, F.F., Deng, F.G.: Hyperentanglement concentration for two-photon four-qubit systems with linear optics. Phys. Rev. A **88**, 012302 (2013)
36. Li, T., Long, G.L.: Hyperparallel optical quantum computation assisted by atomic ensembles embedded in double-sided optical cavities. Phys. Rev. A **94**, 022343 (2016)
37. Wei, H.R., Deng, F.G., Long, G.L.: Hyper-parallel Toffoli gate on three-photon system with two degrees of freedom assisted by single-sided optical microcavities. Opt. Express **24**, 18619 (2016)
38. Nemoto, K., Munro, W.J.: Nearly deterministic linear optical controlled-NOT gate. Phys. Rev. Lett. **93**, 250502 (2004)
39. Hofmann, H.F.: Quantum computing with cross-Kerr nonlinearities. Phys. Rev. A **72**, 022329 (2005)
40. Brod, D.J., Combes, J.: A passive CPHASE gate via cross-Kerr nonlinearities. Phys. Rev. Lett. **117**, 080502 (2016)
41. Dong, L., Yang, M., Cao, Z.L., Zhang, Z.J.: Single-photon controlled multi-photon polarization unitary gate based on weak cross-Kerr nonlinearities. Quantum Inf. Process. **17**, 114 (2018)
42. Wang, M., Yan, F., Gao, T.: Generation of four-photon polarization entangled decoherence-free states with cross-Kerr nonlinearity. Sci. Rep. **6**, 38233 (2016)
43. Dong, L., Yang, M., Cao, Z.L., Zhang, Z.J.: Nearly deterministic preparation of the perfect W state with weak cross-Kerr nonlinearities. Phys. Rev. A **93**, 012308 (2016)
44. Xiu, X.M., Yuan, J.B., Liu, Y.M., Zhou, L.: Preparation of four-photon polarization-entangled decoherence-free states employing weak cross-Kerr nonlinearities. Phys. Rev. A **94**, 042321 (2016)
45. Shen, C.P., Liang, L.M., Oh, C.H.: Multiphoton Knill-Laflamme-Milburn states generated by nonlinear optics. J. Opt. Soc. Am. B **35**, 694–701 (2018)
46. Barrett, S.D., Kok, P., Nemoto, K., Beausoleil, R.G., Munro, W.J., Spiller, T.P.: Symmetry analyzer for nondestructive Bell-state detection using weak nonlinearities. Phys. Rev. A **71**, 060302(R) (2005)
47. Sheng, Y.B., Deng, F.G., Zhou, H.Y.: Nonlocal entanglement concentration scheme for partially entangled multipartite systems with nonlinear optics. Phys. Rev. A **77**, 062325 (2008)
48. Guo, Q., Wang, J., Fan, H.: Simplified optical quantum-information processing via weak cross-Kerr nonlinearities. Phys. Rev. A **83**, 054303 (2011)
49. Cao, T.B., Nguyen, B.A.: Bidirectional remote hyperstate preparation under common quantum control using hyperentanglement. J. Opt. Soc. Am. B **40**, 11 (2023)
50. Ma, P.-C., Chen, G.-B., Hu, B.-L., Shi, J., Yu, X., Zhan, Y.-B.: Bidirectional controlled remote implementation of quantum operations. Laser Phys. Lett. **22**, 125204 (2025)

Publisher's Note Springer Nature remains neutral with regard to jurisdictional claims in published maps and institutional affiliations.

Springer Nature or its licensor (e.g. a society or other partner) holds exclusive rights to this article under a publishing agreement with the author(s) or other rightsholder(s); author self-archiving of the accepted manuscript version of this article is solely governed by the terms of such publishing agreement and applicable law.